

# Synthesis and structure of the tetradeca-iron(III) oxide–alkoxide cluster $[\text{Bu}_4\text{N}]_2[\text{Fe}_{14}\text{O}_8(\text{OCH}_2\text{CH}_3)_{20}\text{Cl}_8]$

Craig A. Grapperhaus<sup>\*</sup>, Martin G. O'Toole, Mark S. Mashuta

Department of Chemistry, University of Louisville, 2320 So. Brook St., Louisville, KY 40292, United States

Received 26 June 2006; accepted 25 July 2006

Available online 2 August 2006

## Abstract

The iron(III) oxide–alkoxide cluster, di-tetra-*n*-butylammonium octachloro-tetra( $\mu_3$ -oxo)-tetra( $\mu_4$ -oxo)- icos( $\mu_2$ -ethoxo)-tetradeca-iron(III), has been isolated and its X-ray crystal structure determined.

© 2006 Elsevier B.V. All rights reserved.

**Keywords:** Iron; Oxo compounds; Alkoxides; Cluster compounds; Sulfur; Oxidation; Oxygen

The oxidation of iron compounds to iron oxides is a well known, yet complex process. During our studies of the oxygen sensitivity of iron–thiolate complexes, we reproducibly generate an insoluble orange powder upon exposure of  $\text{LFeCl}$  (**1**) ( $\text{L} = 4,7\text{-bis}(2'\text{-methyl-2'-mercaptopropyl})\text{-1-thia-4,7-diazacyclononane}$ ) to dioxygen in solution [1,2]. The oxidation product is insoluble in all common solvents preventing full spectroscopic characterization, but it displays a diagnostic IR spectrum. Similar products were reported by others studying iron–thiolate oxygen sensitivity, but the product was never fully characterized [3–6]. Herein we report the isolation and structure of the iron(III) oxide–alkoxide cluster,  $[\text{Bu}_4\text{N}]_2[\text{Fe}_{14}\text{O}_8(\text{OCH}_2\text{CH}_3)_{20}\text{Cl}_8]$  (**2**).

Complex **2** is the largest iron(III) oxide–alkoxide cluster known to date. Previously, clusters with 5–10 iron centers have been isolated and structurally characterized [7–15]. Typically, these clusters are derived from iron(III) chloride and the appropriate alkoxide. Chloride from the iron source may be present or absent in the product. These clusters have been studied for a variety of reasons including their magnetic properties [8,14,15] and application to homogenous catalysis [7,9–11]. Very recently, XAS data

on whole blood cells from *Perophora annectens* reveal the presence of an iron alkoxide cluster,  $[\text{Fe}_4\text{-}\mu\text{-(OR)}_5(\text{OR})_{9-10}]$  [16].

Previously, we reported the synthesis of **1** from  $\text{H}_2\text{L}$ ,  $\text{NEt}_3$ , and  $[\text{NBu}_4][\text{FeCl}_4]$  in ethanol [1]. Complex **1** precipitates as a blue solid, which is isolated by filtration leaving a dark brown filtrate. The filtrate was allowed to stand in air over a period of several days yielding **2** as orange block shaped crystals with an infrared spectrum identical to the oxidation product of **1**. The structure of **2** was determined by X-ray crystallography [17–22].

Compound **2** crystallizes in the tetragonal space group  $P4_2/c$  with  $a = 17.0996(10)$  Å and  $c = 21.027(3)$  Å.<sup>1</sup> Since crystals of **2** rapidly degrade upon removal from the mother liquor, all manipulations were preformed in a cold room. Numerous crystals were selected and mounted in an attempt to obtain a more precise crystal structure, however a higher quality data set could not be obtained. The data

<sup>1</sup> Crystal data for **1**:  $[\text{Bu}_4\text{N}]_2[\text{Fe}_{14}\text{O}_8(\text{OCH}_2\text{CH}_3)_{20}\text{Cl}_8]$ ,  $FW = 2579.62$  g mol<sup>−1</sup> tetragonal, space group  $P4_2/c$ ,  $a = 17.0996(10)$  Å,  $c = 21.027(3)$  Å,  $V = 6148.1(9)$  Å<sup>3</sup>,  $Z = 2$ ,  $\mu = 1.827$  mm<sup>−1</sup>,  $\rho = 1.393$  g cm<sup>−3</sup>. Data were collected on a Bruker Smart Apex CCD using Mo K $\alpha$  radiation. For all 5447 unique reflections ( $R(\text{int}) = 0.2003$ ), the final anisotropic full-matrix least-squares refinement on  $F^2$  for 240 variables data converged at  $R_1 = 0.1018$  and  $wR_2 = 0.2276$  with a GOF of 1.075.

<sup>\*</sup> Corresponding author. Tel.: +1 502 852 5932; fax: +1 502 852 8149.  
E-mail address: [grapperhaus@louisville.edu](mailto:grapperhaus@louisville.edu) (C.A. Grapperhaus).

set was collected at low temperature, 100 K. A representation of the  $[\text{Fe}_{14}\text{O}_8(\text{OCH}_2\text{CH}_3)_{20}\text{Cl}_8]^{2-}$  dianion is shown in Fig. 1.

Compound **2** contains four unique iron centers, labeled  $\text{Fe}1^a$ ,  $\text{Fe}2^a$ ,  $\text{Fe}3^a$ , and  $\text{Fe}4^a$  (Fig. 1). There are 10 additional symmetry generated iron centers. The seven unique oxygen atoms include five  $\mu_2$ -ethoxides ( $\text{O}1^a$ – $\text{O}5^a$ ), a  $\mu_3$ -oxo ( $\text{O}6^a$ ), and a  $\mu_4$ -oxo ( $\text{O}7^a$ ). For each O-donor, symmetry generates three additional sites. The  $\text{Fe}$ – $\text{OC}_2\text{H}_5$  bond distances (Table 1) fall in the range of 1.946(11)–2.051(10) Å with an average of 2.00(1) Å that is identical within error to a previously reported  $\text{Fe}$ – $\text{OC}_2\text{H}_5$  ( $\mu_2$ ) distance of 2.009(1) Å [14]. The  $\text{Fe}$ – $\lambda^3\text{O}$  distances fall within error of related structures, 1.911(1) Å, and range from 1.853(10) to 1.954(9) Å with an average of 1.91(1) Å [14]. The  $\text{Fe}$ – $\lambda^4\text{O}$  distances vary from 1.962(9) to 2.097(10) Å, with an average of 2.00(1) Å near the reported value of 2.011(7) Å [14]. The cluster also contains two unique terminal chlorides,  $\text{Cl}1^a$  and  $\text{Cl}2^a$ , and six additional symmetry generated chlorides. The  $\text{Fe}1$ – $\text{Cl}1$  and  $\text{Fe}2$ – $\text{Cl}2$  distances of 2.341(4) and 2.241(5) Å are within the expected range. Overall, the dianion of **2** contains a cluster of 14 iron centers, 20  $\mu_2$ -ethoxides, four  $\mu_3$ -oxo bridges, four  $\mu_4$ -oxo bridges, and eight terminal chlorides. Based on charge balance, each iron exists in the ferric state.

The 14 iron centers of **2** are arranged in a pair of point-sharing  $\text{Fe}_7$ -ditetrahedra (Fig. 2). An  $\text{Fe}_4$ -tetrahedron can

Table 1  
Selected bond distances (Å) for **2**

$\text{Fe}1^a$ – $\text{O}1^a$	2.093(9)	$\text{Fe}3^a$ – $\text{O}3^a$	2.010(10)
$\text{Fe}1^a$ – $\text{O}4^a$	1.971(10)	$\text{Fe}3^a$ – $\text{O}4^a$	2.051(10)
$\text{Fe}1^a$ – $\text{O}5^a$	1.952(10)	$\text{Fe}3^a$ – $\text{O}7^d$	1.973(9)
$\text{Fe}1^a$ – $\text{O}6^b$	1.954(9)		
$\text{Fe}1^a$ – $\text{O}7^d$	2.097(10)	$\text{Fe}4^d$ – $\text{O}2^a$	2.047(10)
$\text{Fe}1^a$ – $\text{Cl}1^a$	2.341(4)	$\text{Fe}4^d$ – $\text{O}5^d$	1.976(9)
$\text{Fe}2^a$ – $\text{O}1^a$	1.956(11)	$\text{Fe}4^d$ – $\text{O}6^a$	1.853(10)
$\text{Fe}2^a$ – $\text{O}2^a$	1.946(11)	$\text{Fe}4^d$ – $\text{O}6^d$	1.924(10)
$\text{Fe}2^a$ – $\text{O}3^a$	1.953(11)	$\text{Fe}4^d$ – $\text{O}7^d$	1.962(9)
$\text{Fe}2^a$ – $\text{O}7^d$	1.992(9)		
$\text{Fe}2^a$ – $\text{Cl}2^a$	2.241(5)		

be formed with  $\text{Fe}1^a$ ,  $\text{Fe}2^a$ ,  $\text{Fe}3^a$ , and  $\text{Fe}4^d$ .  $\text{Fe}3^a$  sits on the special position (0.5,0.5, $z$ ) and serves as the joining point for the second tetrahedron, which also contains  $\text{Fe}1^c$ ,  $\text{Fe}2^c$ , and  $\text{Fe}4^b$ . The tetrahedra are also connected by  $\text{O}6$  linkages between  $\text{Fe}1^c/\text{Fe}4^d$  and  $\text{Fe}1^a/\text{Fe}4^b$ . The  $\text{O}6$  linkage also extends out to  $\text{Fe}4$  positions in the second  $\text{Fe}_7$ -ditetrahedra, which sits across the cluster and perpendicular to the first. The two  $\text{Fe}_7$  cores are also linked together by four  $\mu_2$ -ethoxides, consisting of  $\text{Fe}1^a$ ,  $\text{O}5^a$ , and  $\text{Fe}4^a$  and their symmetry generated equivalents.

An isolated  $\text{Fe}_4$ -tetrahedron is shown in Fig. 3. As shown,  $\text{Fe}2^a$  sits atop of the tetrahedron in a trigonal bipyramidal environment with  $\mu_2$ -ethoxides in all three equatorial positions. The ethoxides  $\text{O}1^a$ ,  $\text{O}2^a$ , and  $\text{O}3^a$  bridge the

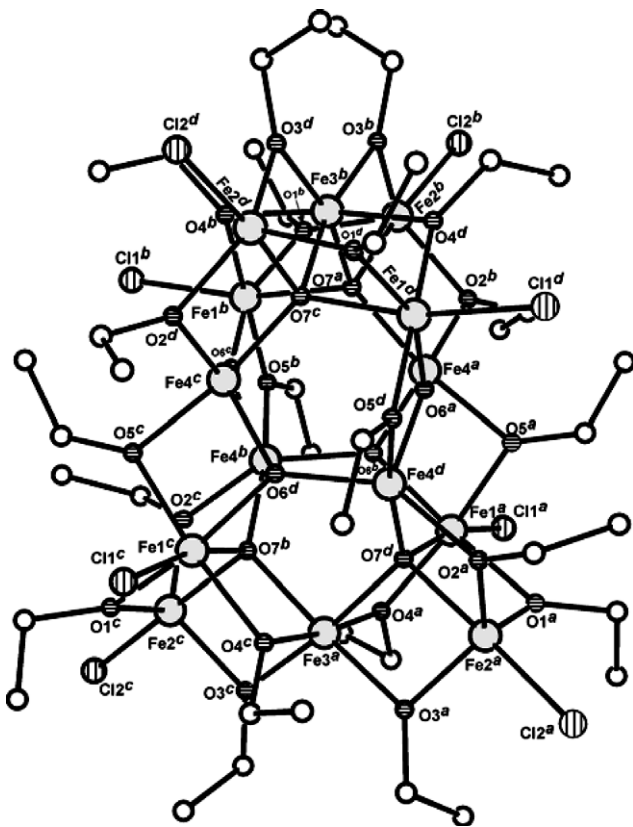


Fig. 1. A PLUTO representation of the dianion of **2**. The atoms from the asymmetric unit are labeled as  $a$ . Other positions are symmetry generated;  $b$  ( $y, 1-x, -z$ ),  $c$  ( $1-x, 1-y, z$ ),  $d$  ( $1-y, x, -z$ ).

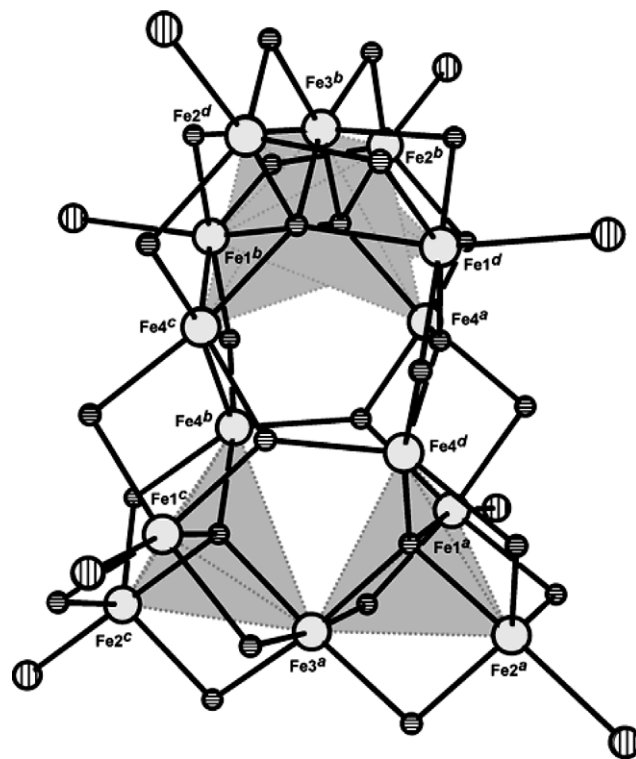


Fig. 2. A PLUTO representation of the dianion of **2**. Carbon atoms have been omitted. The  $\text{Fe}_7$ -ditetrahedra are outlined in gray. The atoms from the asymmetric unit are labeled as  $a$ . Other positions are symmetry generated;  $b$  ( $y, 1-x, -z$ ),  $c$  ( $1-x, 1-y, z$ ),  $d$  ( $1-y, x, -z$ ).

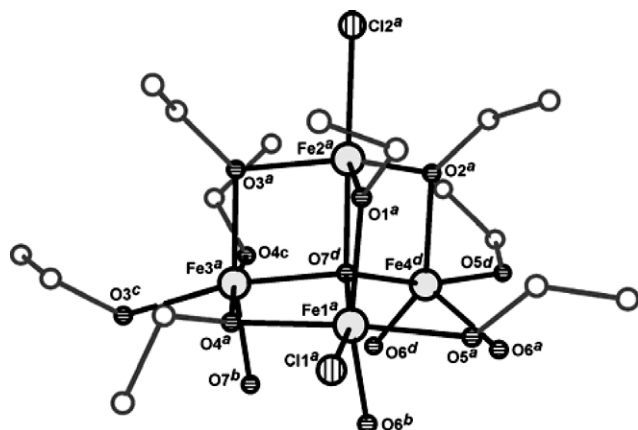


Fig. 3. A PLUTO representation of a  $\text{Fe}_4$ -tetrahedron from **2**. The atoms from the asymmetric unit are labeled as *a*. Other positions are symmetry generated; *b* ( $y, 1-x, -z$ ), *c* ( $1-x, 1-y, z$ ), *d* ( $1-y, x, -z$ ).

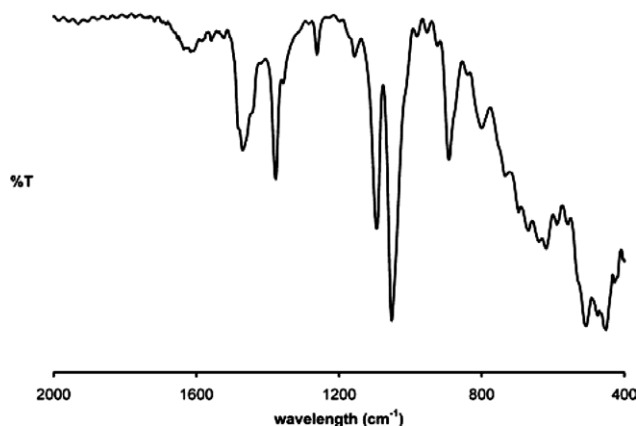


Fig. 4. Infrared spectrum of **2** prepared as a KBr pellet at  $4\text{ cm}^{-1}$  resolution.

$\text{Fe}2^a\text{--Fe}1^a$ ,  $\text{Fe}2^a\text{--Fe}3^a$ , and  $\text{Fe}2^a\text{--Fe}4^d$  edges of the tetrahedron, respectively. A terminal chloride,  $\text{Cl}2^a$ , and a  $\mu_4$ -oxo,  $\text{O}7^d$ , sit in the axial positions of  $\text{Fe}2^a$ . All four iron centers are coordinated to  $\text{O}7^d$ , which is located on the interior of the  $\text{Fe}_4$ -tetrahedron. A fourth  $\mu_2$ -ethoxide,  $\text{O}4^a$ , sits along the  $\text{Fe}1^a\text{--Fe}3^a$  edge. The pseudo-octahedral environment about  $\text{Fe}3^a$  is completed by the symmetry generated equivalents  $\text{O}3^c$ ,  $\text{O}4^c$ , and  $\text{O}7^b$  in the adjoining point-sharing  $\text{Fe}_4$ -tetrahedron. The environment around  $\text{Fe}1^a$  is completed by  $\text{O}6^b$ , a  $\mu_3$ -oxo bridge, which joins a single  $\text{Fe}1$  with two  $\text{Fe}4$  sites. A  $\mu_2$ -ethoxy bridge,  $\text{O}5$ , between  $\text{Fe}1$  and  $\text{Fe}4$  completes a diamond core and the coordination environment of  $\text{Fe}1$  and  $\text{Fe}4$ .

The infrared spectrum of **2** is shown in Fig. 4. The IR shows weak bands at  $457$  and  $511\text{ cm}^{-1}$ , which are similar to those in  $\alpha\text{-Fe}_2\text{O}_3$  [23]. The more intense bands at  $806$  and  $893\text{ cm}^{-1}$  are consistent with the presence of alkoxide in the sample. This is further confirmed by the array of bands at  $1053$ ,  $1095$ ,  $1379$ , and  $1471\text{ cm}^{-1}$  [12]. Finally, C–H bending modes are observed at  $2875$ ,  $2929$ , and  $2960\text{ cm}^{-1}$  (not shown).

In conclusion, the orange, insoluble product from the oxidation of iron–thiolate complexes in alcohol has been

identified as an iron(III) oxo-alkoxide cluster. The tetradecairon(III) cluster has an IR spectrum consistent with the thiolate oxidation product upon oxidation of the filtrate from the synthesis of **1**. This cluster, **2**, is the largest member of the growing family of iron(III) oxo-alkoxides.

## Acknowledgement

Acknowledgment is made to the National Science Foundation (CHE-0238137) for funding provided to C.A.G. CCD X-ray equipment was purchased through funds provided by the Kentucky Research Challenge Trust Fund.

## Appendix A. Supplementary data

Supplementary data associated with this article can be found, in the online version, at [doi:10.1016/j.inoche.2006.07.027](https://doi.org/10.1016/j.inoche.2006.07.027).

## References

- [1] C.A. Grapperhaus, M. Li, A.K. Patra, S. Poturovic, P.M. Kozlowski, M.Z. Zgierski, M.S. Mashuta, *Inorg. Chem.* 42 (2003) 4382–4388.
- [2] C.A. Grapperhaus, M.G. O'Toole, unpublished results.
- [3] T.C. Harrop, P.K. Mascharak, *Acc. Chem. Res.* 37 (2004) 253–260.
- [4] C.M. Lee, C.H. Hsieh, A. Dutta, G.H. Lee, W.F. Liaw, *J. Am. Chem. Soc.* 125 (2003) 11492–11493.
- [5] C.M. Lee, C.H. Chen, H.W. Chen, J.L. Hsu, G.H. Lee, W.F. Liaw, *Inorg. Chem.* 44 (2005) 6670–6679.
- [6] R.M. Theisen, J. Shearer, W. Kaminsky, J.A. Kovacs, *Inorg. Chem.* 43 (2004) 7682–7690.
- [7] S. Asirvatham, M.A. Khan, K.M. Nicholas, *Inorg. Chem.* 39 (2000) 2006–2007.
- [8] H.K. Chae, C. Hwang, Y. Dong, H. Yun, H.G. Jang, *Chem. Lett.* (2000) 992–993.
- [9] K. Hegetschweiler, H. Schmalke, H.M. Streit, W. Schneider, *Inorg. Chem.* 29 (1990) 3625–3627.
- [10] K. Hegetschweiler, H.W. Schmalke, H.M. Streit, V. Gramlich, H.U. Hund, I. Erni, *Inorg. Chem.* 31 (1992) 1299–1302.
- [11] B.J. O'Keefe, S.M. Monnier, M.A. Hillmyer, W.B. Tolman, *J. Am. Chem. Soc.* 123 (2001) 339–340.
- [12] G.A. Seisenbaeva, S. Gohil, E.V. Suslova, T.V. Rogova, N.Y. Turova, V.G. Kessler, *Inorg. Chim. Acta* 358 (2005) 3506–3512.
- [13] J. Spandl, M. Kusserow, I. Brudgam, *Z. Anorg. Allg. Chem.* 629 (2003) 968–974.
- [14] M. Veith, F. Gratz, V. Huch, *Eur. J. Inorg. Chem.* (2001) 367–368.
- [15] M. Veith, F. Gratz, V. Huch, P. Gutlich, A. Ensling, *Z. Anorg. Allg. Chem.* 630 (2004) 2329–2336.
- [16] P. Frank, A. DeTomaso, B. Hedman, K.O. Hodgson, *Inorg. Chem.* 45 (2006) 3290–3293.
- [17] SMART (v.5628), Bruker Advanced X-ray Solutions, Inc., Madison, WI, 2002.
- [18] SAINT (v6.36), Bruker Advanced X-ray Solutions, Inc., Madison, WI, 2002.
- [19] G.M. Sheldrick, SADABS (v2.02), University Gottingen, Gottingen, Germany, 2001.
- [20] G.M. Sheldrick, SHELXS-90, *Acta Crystallogr. A* 46 (1990) 467.
- [21] G.M. Sheldrick, SHELXL-97, University Gottingen, Gottingen, Germany, 1997.
- [22] SHELXTL (v6.12), Bruker Advanced X-ray Solutions, Inc. Madison, WI (2001).
- [23] R. Balasubramaniam, A.V.R. Kumar, *Corros. Sci.* 45 (2003) 2451–2465.